Thermal Neutron Scattering Measurements of YH_x for the Transformational Challenge Reactor[1]

Chris W. Chapman*, Xunxiang Hu*, Jesse Brown*, Goran Arbanas*, Alexander I. Kolesnikov*, Yongqiang Cheng*, and Luke Daemen*

*Oak Ridge National Laboratory, 1 Bethel Valley Road, Oak Ridge, TN, 37831
chapmancw@ornl.gov

INTRODUCTION

The Transformational Challenge Reactor (TCR) targets application of advances in manufacturing, materials, and computational sciences to accelerate development of new nuclear reactor technologies as well as their adoption by the U.S. industry [1]. The TCR leverages advanced manufacturing capabilities at Oak Ridge National Laboratory (ORNL) to facilitate an agile reactor design with the ability to take advantage of advanced materials and data science-informed certification schemes. Since TCR is gas-cooled a thermal reactor, the choice of neutron moderating material is of crucial importance. To achieve a highly efficient and compact core while minimizing the amount of high assay low enriched uranium required [2], a hydrogen-bearing moderator that is stable to high temperatures is required. This initially led to the selection of metal hydrides (i.e., ZrH_x and YH_x) for the TCR demonstration core.

ZrH_x has been extensively studied and used in previous reactor designs since the 1950s due to its low absorption cross section and general availability [3]. However, during the same period, the unavailability of high-purity yttrium as an industrial metal barred it from being considered as another candidate although it exhibits advantageous thermal stability compared to ZrH_x [4, 5]. Today yttrium metal of high purity is available as an industrial metal and therefore, YH_x was chosen as the moderator material for the TCR. However, a complete thermal scattering library is currently lacking and is needed for an accurate representation of TCR core neutronics properties. This paper details the first step towards the evaluation of a YH_x thermal scattering library through the conduct of thermal neutron scattering experiments for various hydrogen atomic concentrations x = 1.62, 1.74, 1.85, 1.90 at 5 Kelvin and room temperature at the Spallation Neutron Source (SNS) at ORNL. This information supplies the necessary data for TCR's YH_x moderator while providing basic information that is necessary for design and deployment of any other reactor taking advantage of this high performance moderator.

YTTRIUM HYDRIDE

Yttrium hydride offers unique advantages as a moderator for thermal nuclear reactors. In contrast to other hydrides under consideration, this material retains its relatively high content of hydrogen at elevated temperatures. For example, the hydrogen pressure required to maintain the thermodynamic equilibrium of $YH_{1.7}$ is 2.5–4.5 orders of magnitude lower than that of $ZrH_{1.7}$ at the same temperatures, indicating that YHx has superior thermal stability over ZrHx.

The application of ZrHx in nuclear systems required careful management of the moderator temperature and additional effort to develop a hydrogen barrier to mitigate hydrogen desorption at elevated temperatures. In contrast, the thermodynamic driving force for H desorption from YHx is significantly smaller and results in its stability at elevated temperatures.

The yttrium hydride was manufactured at ORNL's Low Activation Materials Development and Analysis laboratory. This was done by introducing specific amounts of hydrogen into a small volume of yttrium that was kept in a vacuum [6]. This allowed for production of complex geometries of YH_x metals without cracking. The H/Y ratio was determined by the weight change of the yttrium sample before and after inserting hydrogen.

THERMAL NEUTRON SCATTERING THEORY

Double differential thermal neutron scattering is described by,

$$\frac{d^2\sigma}{d\Omega dE_f} = \frac{\sigma_b}{4\pi k_B T}\sqrt{\frac{E_f}{E_i}}e^{\frac{-\beta}{2}}S\left(\alpha,\beta\right), \tag{1}$$

where σ_b is the bound scattering cross section, k_B is the Boltzmann constant, $E_{i,f}$ are the incident and final neutron energies, respectively, and $S\left(\alpha,\beta\right)$ is the thermal scattering law where α and β are dimensionless quantities corresponding to momentum and energy transfer as defined by,

$$\alpha = \frac{E_i + E_f - 2\mu\sqrt{E_i E_f}}{Ak_B T}, \quad \beta = \frac{E_f - E_i}{k_B T}, \tag{2}$$

where μ is the cosine of the scattering angle in the laboratory system, and A is the ratio of the mass of the scattering atom to the mass of the neutron. The thermal scattering law is defined by the dynamic structure factor in,

$$S\left(\alpha,\beta\right) = k_B T e^{\frac{E}{2k_B T}} S(Q,E), \tag{3}$$

where $S(Q,E)$ is the dynamic structure factor defined by momentum transfer $\hbar Q$ (where $\hbar$ is the reduced Planck constant) and energy transfer $E = E_i - E_f$.

There are several ways to calculate the dynamic structure factor (as described in Refs. [7, 8]). The most common involves using the LEAPR module of NJOY [9], which generates the thermal scattering law from using the phonon density

of states or crystallographic structure information as needed. The phonon density of states is used to calculate incoherent scattering, while the crystallographic structure information is used to calculate coherent scattering. Both are needed to fully describe the thermal scattering law of YH_x.

EXPERIMENTAL RESULTS

Experimental data were gathered at the SNS from two instruments: the Fine-Resolution Fermi Chopper Spectrometer, SEQUOIA [10], and the Vibrational Spectrometer VISION [11].

SEQUOIA

To measure the double differential scattering cross section, the time-of-flight direct geometry spectrometer SEQUOIA was used. Measurements were taken at three incident neutron energies: 45, 180, and 600 meV. The incident energies of 45 and 180 meV were selected based on previous calculations and measurements of the phonon density of states [12, 13] that show significant phonon density below 30 meV and between 110–145 meV (as shown in Fig. 1). In order to best see these features, the incident neutron energies were chosen to be slightly higher than the location of these peaks to ensure the best resolution, which led to the choice of 45 and 180 meV. The 600 meV incident energy was chosen to measure multi-phonon scattering.

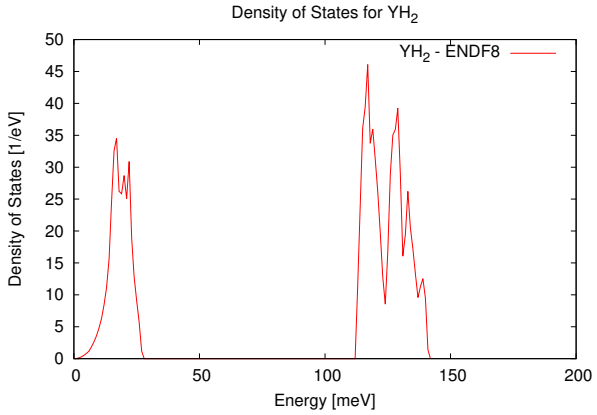

Fig. 1. Phonon density of states of YH_2 from ENDF/B-VIII.0.

Measurements of YH_x, for x = 1.62, 1.85, were taken at temperatures of 5 and 295 K. Experimental results are shown in Figs. 2–5. Figure 2 shows the Q-integrated dynamic structure factor for E_i=45 meV, where the intensity increase at $E < 0$ (corresponding to neutron upscattering) at 295 K is due to the increase of the Bose population factor[7], which is significantly muted at 5 K. Figures 3 and 4 display the E_i=180 meV data in as a 2D mesh of the dynamic structure factor for $YH_{1.85}$ and as a Q-integrated spectra comparing $YH_{1.62}$ and $YH_{1.85}$. The two phonon density peaks shown in Fig. 1 can be seen in both of these figures. Specifically, the contribution from the phonon density of states peaks can be seen in the yellow patch just above the elastic line around E=15 meV and between 100 and 150 meV. The former corresponding to the yttrium vibration in the lattice, while the latter is from hydrogen vibration in the lattice.

There is also an anharmonicity above E=400 meV which can be seen in the Q-integrated dynamic structure factor for the E_i=600 meV plot in Fig. 5, based on calculated multiphonon neutron scattering in harmonic approximation using the spectra shown in Fig. 4 (see below discussion on VISION data). This is an expected feature of YH_x, and careful analysis will be required to completely model this effect. Analysis of the SEQUOIA data is ongoing, and high temperature measurements up to 800 K are scheduled for later this year. Measurements up to 1,500 K are scheduled at the Wide Angular-Range Chopper Spectrometer (ARCS) later this year, as well.

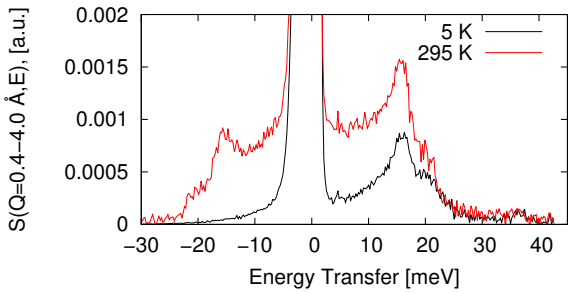

Fig. 2. Temperature comparison of Q-integrated dynamic structure factor of $YH_{1.85}$ for E_i=45 meV at 5 K and 295 K.

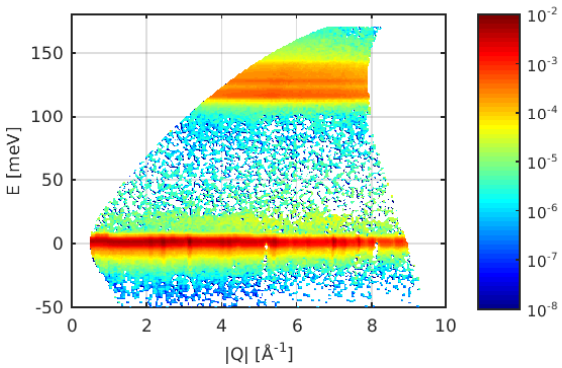

Fig. 3. 2D mesh of the dynamic structure factor of $YH_{1.85}$ for E_i=180 meV at 5 K.

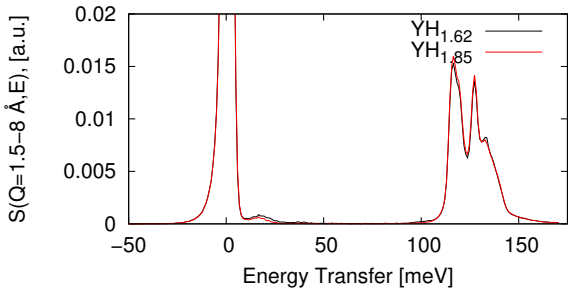

Fig. 4. Hydrogen concentration of Q-integrated dynamic structure factor of $YH_{1.62}$ and $YH_{1.85}$ for E_i=180 meV at 5 K.

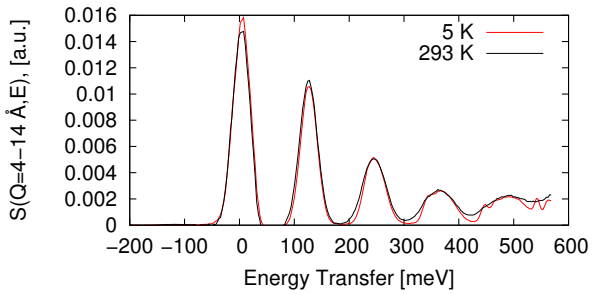

Fig. 5. Q-integrated dynamic structure factor of $YH_{1.85}$ for E_i=600 meV at 5 K and 293K.

VISION

To study the vibrational features of YH_x, the indirect geometry VISION instrument was used. VISION shines a white beam of neutrons (wide distribution of incident neutron energies), and the final energy is set to 4 meV. This allows for an analysis of the whole energy range of interest (up to 1 eV), with a constant relative energy resolution of $\Delta E/E = 1.5\%$. Experimental results for YH_x, where $x = 1.62, 1.74, 1.85, 1.90$ for forward scattering (45°) and backscattering (135°) at 5 K, are shown in Figs. 6 and 7, respectively, while a comparison of the $YH_{1.85}$ results at 5 and 293 K are shown in Figs. 9 and 10.

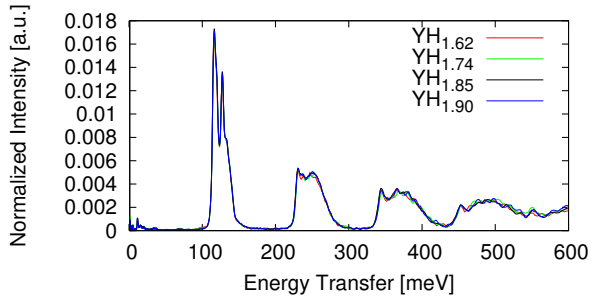

Fig. 6. Hydrogen concentration comparison of forward scattering data of YH_x, for $x = 1.62, 1.74, 1.85, 1.90$ at 5K.

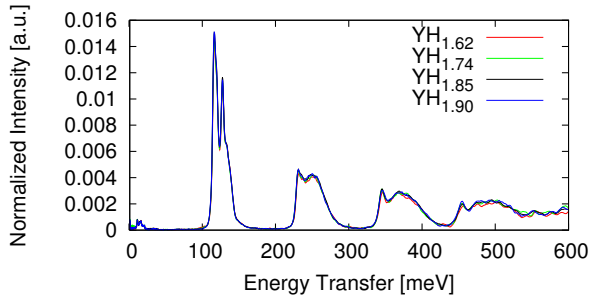

Fig. 7. Hydrogen concentration comparison of backscattering data of YH_x, for $x = 1.62, 1.74, 1.85, 1.90$ at 5K.

Because of the constant relative energy resolution, the full energy spectrum can be more easily seen in Figs. 6 and 7. The magnitude and location of the vibrational modes are very similar across the four samples. There is evidence to suggest that potential well for hydrogen in yttrium is anharmonic at energies higher than 300 meV. There is a significant red-shift of the lower peaks in the 3-, 4- and 5-multiphonon bands compared to the multiphonon INS spectra calculated in harmonic approximation [14] and the Sjölander approximation for higher order multiphonon scattering [15] using experimental spectra in the range of fundamental modes, E<160 meV, as shown in Fig. 8. The temperature comparisons in Figs. 9 and 10 show the effects of this anharmonicity as a function of temperature. As with the SEQUOIA data, analysis of the VISION data is ongoing.

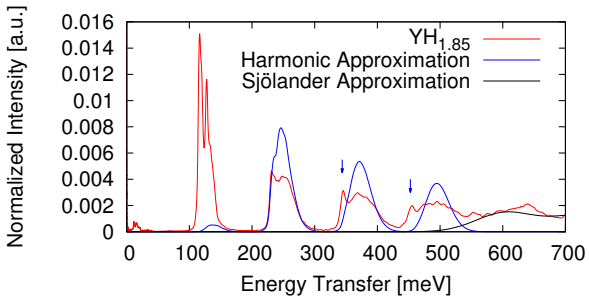

Fig. 8. Comparison of VISION backscattering 5K experimental data with multiphonon harmonic and Sjölander approximations.

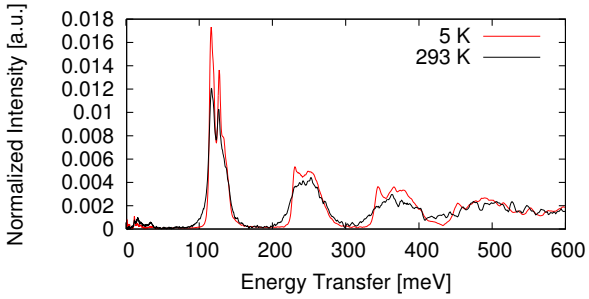

Fig. 9. Forward scattering data of $YH_{1.85}$ at 5 K and 293 K.

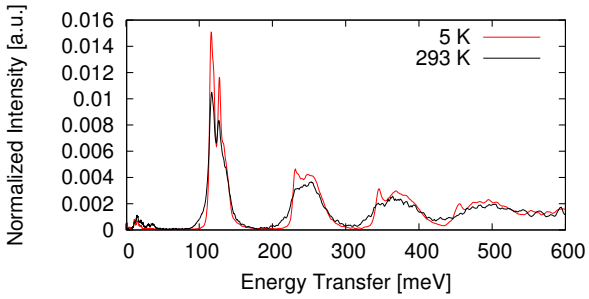

Fig. 10. Backscattering data of $YH_{1.85}$ at 5 K and 293 K.

CONCLUSIONS AND FUTURE WORK

Thermal neutron scattering measurements of YH_x for hydrogen concentrations $x = 1.62, 1.74, 1.85, 1.90$ at 5 K and room temperature were conducted at the SEQUOIA and VISION beamlines of the SNS for use in the TCR. There are

small differences in the spectra, which could be due to the non-uniform hydration of the samples. This will be confirmed with x-ray diffraction measurements.

Analysis of the experimental data is ongoing, with the result being a thermal scattering law for YH_x depending on the final choice of hydrogen concentration x for use in the TCR. Computational simulations of the YH_x samples using density functional theory (DFT) codes (i.e., CASTEP [16] or VASP [17, 18, 19]) will be used to replicate the data at VISION, while Monte Carlo neutron transport programs will replicate the direct-geometry spectrometer results from SEQUOIA.

ACKNOWLEDGMENTS

This research was sponsored by the Transformational Challenge Reactor Program of the US Department of Energy Office of Nuclear Energy. This research used resources at the Spallation Neutron Source, a DOE Office of Science User Facility operated by the Oak Ridge National Laboratory.

REFERENCES

1. *Transformational Challenge Reactor, (n.d.)*, tcr.ornl.gov.
2. B. ADE, A. WYSOCKI, B. BETZLER, M. GREENWOOD, P. CHESSER, P. JAIN, J. BURNS, K. TERRANI, J. RADER, B. HISCOX, J. HEINEMAN, J. RISNER, K. SMITH, F. HEIDET, A. BERGERON, J. STERBENTZ, T. HOLSCHUH, and N. BROWN, "Candidate Core Designs for the Transformational Challenge Reactor," In: Proc. PHYSOR 2020, Cambridge, UK, 2020.
3. W. MUELLER, J. BLACKLEDGE, and G. LIBOWITZ, *Metal Hydrides*, Academic Press (1968).
4. W.-E. WANG and D. R. OLANDER, "Thermodynamics of the Zr-H System," *Journal of the American Ceramic Society*, **78**, *12*, 3323–3328 (1995).
5. G. M. BEGUN, J. F. LAND, and J. T. BELL, "High temperature equilibrium measurements of the yttrium-hydrogen isotope (H2, D2, T2) systems." *The Journal of Chemical Physics*, **72**, *5*, 2959–2966 (1980).
6. R. V. HOUTEN, *United States Patent No. 3720751* (1973), retrieved from https://patentimages.storage.googleapis.com/bc/6d/62/b9ab3810817ce3/US3720751.pdf.
7. D. L. PRICE and F. FERNANDEZ-ALONSO, *Neutron Scattering - Fundamentals*, Academic Press, 1st ed. (2013).
8. G. SQUIRES, *Thermal Neutron Scattering*, Cambridge University Press., 3rd ed. (1978).
9. R. MACFARLANE and A. KAHLER, "Methods for Processing ENDF/B-VII with NJOY," *Nuclear Data Sheets*, **111**, *12*, 2739–2890 (2010), Nuclear Reaction Data.
10. G. E. GRANROTH, A. I. KOLESNIKOV, T. E. SHERLINE, J. P. CLANCY, K. A. ROSS, J. P. C. RUFF, B. D. GAULIN, and S. E. NAGLER, "SEQUOIA: A Newly Operating Chopper Spectrometer at the SNS," *Journal of Physics: Conference Series*, **251**, 012058 (Nov 2010).
11. P. A. SEEGER, L. L. DAEMEN, and J. Z. LARESE, "Resolution of VISION, a Crystal-Analyzer Spectrometer," *Nuclear Instruments and Methods in Physics Research Section A: Accelerators, Spectrometers, Detectors and Associated Equipment*, **604**, *3*, 719 – 728 (2009).
12. ZERKLE, MICHAEL and HOLMES, JESSE, "A Thermal Neutron Scattering Law for Yttrium Hydride," *EPJ Web Conf.*, **146**, 13005 (2017).
13. T. J. UDOVIC, J. J. RUSH, and I. S. ANDERSON, "Local-mode dynamics in YH_2 and YD_2 by isotope-dilution neutron spectroscopy," *Phys. Rev. B*, **50**, 15739–15743 (Dec 1994).
14. J. LI and A. KOLESNIKOV, "Neutron spectroscopic investigation of dynamics of water ice," *Journal of Molecular Liquids*, **100**, *1*, 1 – 39 (2002).
15. A. SJÖLANDER, "Multi-phonon Processes in Slow Neutron Scattering by Crystals," *Arkiv för Fysik*, **14**, *4*, 315–371 (1958).
16. S. J. CLARK, M. D. SEGALL, C. J. PICKARD, P. J. HASNIP, M. J. PROBERT, K. REFSON, and M. PAYNE, "First principles methods using CASTEP," *Z. Kristall.*, **220**, 567–570 (2005).
17. G. KRESSE and J. HAFNER, "Ab initio molecular dynamics for liquid metals," *Phys. Rev. B*, **47**, 558–561 (Jan 1993).
18. G. KRESSE and J. FURTHMÃIJLLER, "Efficiency of ab-initio total energy calculations for metals and semiconductors using a plane-wave basis set," *Computational Materials Science*, **6**, *1*, 15 – 50 (1996).
19. G. KRESSE and J. FURTHMÜLLER, "Efficient iterative schemes for ab initio total-energy calculations using a plane-wave basis set," *Phys. Rev. B*, **54**, 11169–11186 (Oct 1996).